Spectroscopic and Mutational Analysis of the Blue-Light Photoreceptor AppA: A Novel Photocycle Involving Flavin Stacking with an Aromatic Amino Acid†

Brian J. Kraft,[‡,§] Shinji Masuda,[‡,||,⊥] Jun Kikuchi,[#,▽] Vladimira Dragnea,[||] Gordon Tollin,[△] Jeffrey M. Zaleski,[§] and Carl E. Bauer*[,||]

Departments of Biology and Chemistry, Indiana University, Bloomington, Indiana 47405, Graduate School of Integrated Science, Yokohama City University, and Protein Research Group, Genomic Sciences Center, RIKEN Yokohama Institute, Yokohama 230-0045, Japan, and Department of Biochemistry and Molecular Biophysics, University of Arizona, Tucson, Arizona 85721

Received March 5, 2003

ABSTRACT: The flavoprotein AppA is a blue-light photoreceptor that functions as an antirepressor of photosynthesis gene expression in the purple bacterium *Rhodobacter sphaeroides*. Heterologous expression studies show that FAD binds to a 156 amino acid N-terminal domain of AppA and that this domain is itself photoactive. A pulse of white light causes FAD absorption to be red shifted in a biphasic process with a fast phase occurring in <1 μs and a slow phase occurring at approximately 5 ms. The absorbance shift was spontaneously restored over a 30 min period, also in a biphasic process as assayed by fluorescence quenching and electronic absorption analyses. Site-directed replacement of Tyr21 with Leu or Phe abolished the photochemical reaction implicating involvement of Tyr21 in the photocycle. Nuclear magnetic resonance analysis of wild-type and mutant proteins also indicates that Tyr21 forms $\pi-\pi$ stacking interactions with the isoalloxazine ring of FAD. We propose that photochemical excitation of the flavin results in strengthening of a hydrogen bond between the flavin and Tyr 21 leading to a stable local conformational change in AppA.

Many photosynthetic organisms use blue light to control growth, development, and optimization of photosystem synthesis. In higher plants, at least two different flavin-containing photoreceptors, phototropin and cryptochrome, mediate blue-light perception that includes deetiolation, photoentrainment of the circadian clock, floral initiation, phototropic curvature, chloroplast relocation, and stomatal opening (reviewed in refs *1* and *2*). A homologue of cryptochrome is also involved in mediating circadian rhythms in *Drosophila* and mice, indicating that blue-light sensing is also important in nonphotosynthetic organisms (*2*).

Recently, we demonstrated that the flavoprotein AppA from the purple bacterium *Rhodobacter sphaeroides* represents a new class of photoreceptor that controls photosynthesis gene expression in response to blue-light intensity, as well as to changes in the cellular redox state (*3*). AppA was shown to mediate these effects by functioning as an antirepressor of the photosynthesis repressor PpsR (*3*). A redox mechanism of AppA-mediated antirepression involves breakage of a disulfide bond in oxidized PpsR through disulfide bond isomerization with reduced AppA (*3*). A blue-light-mediated mechanism of AppA antirepression involves the formation of a stable AppA−$PpsR_2$ antirepressor−repressor complex that inhibits the DNA-binding activity of PpsR. Formation of the AppA−$PpsR_2$ complex is inhibited by blue-light excitation of the flavin in AppA, thereby allowing a tetramer of PpsR to repress photosystem gene expression under high-light intensity (*3*). AppA is therefore a bifunctional regulator that controls photosynthesis gene expression in response to both redox and light excitation states of the cell (*3*).

In vivo and in vitro analyses indicate that AppA contains two domains, a Cys-rich carboxyl-terminal domain that is responsible for the isomerization of a disulfide bond in PpsR (*3*, *4*) and an amino-terminal domain that noncovalently binds the blue-light-absorbing chromophore flavin adenine dinucleotide (FAD)[1] (*3*, *5*). Initial biochemical and photochemical analysis indicated that full-length AppA undergoes a photocycle with blue-light irradiation, causing a long-lived 10 nm red shift of the flavin. Initiation of the photocycle also results in a shape change of AppA, as based on alteration of chromatographic profiles of dark versus blue-light-excited

† This work was supported by NIH Grant GM53940 to C.E.B. and by a postdoctoral fellowship to S.M. from the Japan Society for the Promotion of Science.

* To whom correspondence should be addressed. Phone: (812) 855-6595. Fax: (812) 856-4178. E-mail: cbauer@bio.indiana.edu.

‡ The first two authors contributed equally to this work and should be considered co-first authors.

§ Department of Chemistry, Indiana University.

|| Department of Biology, Indiana University.

⊥ Present address: Photodynamics Research Center, RIKEN, Sendai 980-0845, Japan.

Graduate School of Integrated Science, Yokohama City University.

▽ Protein Research Group, Genomic Sciences Center, RIKEN Yokohama Institute.

△ Department of Biochemistry and Molecular Biophysics, University of Arizona.

[1] Abbreviations: CD, circular dichroism; FAD, flavin adenine dinucleotide; LUMO, lowest unoccupied molecular orbital; NMR, nuclear magnetic resonance; PCR, polymerase chain reaction.

10.1021/bi030055o CCC: $25.00
Published on Web 05/13/2003

AppA and by the inability of blue-light-excited AppA to form a stable AppA−$PpsR_2$ complex (*3*).

In this study, we have undertaken biochemical and mutational analysis of the FAD-binding domain of AppA to study the mechanism of its photocycle. Our findings indicate that the N-terminal FAD-binding domain of AppA itself functions as a blue-light sensor that undergoes a characteristic red-shift photocycle even in the absence of the C-terminal domain. Spectral analysis of wild-type and mutant versions of AppA indicates that the photochemical cycle of AppA most likely involves alterations in hydrogen- (H-) bonding interactions between the alloxazine ring of FAD and the hydroxyl group of Tyr21. These results provide new insights into photochemical reaction mechanisms underlying blue-light perception by a flavoprotein photoreceptor.

EXPERIMENTAL PROCEDURES

Construction of Expression Vectors and Purification of the FAD-Binding Domain of AppA. The N-terminal FAD-binding domain of AppA was overexpressed in *Escherichia coli* using a T7 RNA polymerase-based overexpression system that appended the amino terminus of the truncated protein with a His_6 tag (Novagen). For this construction, the region corresponding to residues 1−156 of AppA was amplified using a polymerase chain reaction (PCR) with *Pfu* DNA polymerase. The upstream and downstream oligonucleotide primers, AppA-F, 5′-GGCATATGCAACACGACCTCGAGGC-3′, and AppA156-R, 5′-GGGAGCTCTCAGACGTCGGAGAGGAAACG-3′, respectively, were designed to contain an *Nde*I restriction site at the start codon and a *Sac*I site downstream of the stop codon (start and stop codons are underlined). Chromosomal DNA from *R. sphaeroides* strain HR was used as a PCR template. The PCR-amplified fragment was first cloned into *Sma*I-digested pUC18 (*6*) and then cloned into the *Nde*I−*Sac*I restriction sites of pET28(a)(+) (Novagen), resulting in the recombinant plasmid pETAppA156.

The Tyr residue at position 21 in AppA was changed to Leu and/or Phe (Y21L and Y21F, respectively) by PCR primer mutagenesis using *Pfu* DNA polymerase as described previously (*7*). The primers used were as follows: PET28-F, 5′-CGATCCCGCGAAATTAATACG-3′; Y21L-F, 5′-GTTTCCTGCTGCCTCCGCAGC CTGG-3′; Y21L-R, 5′-CCAGGCTGCGGAGGCAGCAGGAAAC-3′; Y21F-F, 5′-GTTTCCTGCTGCTTCCGCAGCCTGG-3′; and Y21F-R, 5′-CCAGGCTGCGGAAGCAGCAGGAAAC-3′. Y21L-F, Y21L-R and Y21F-F, Y21F-R are the complementary primer pairs to give Y21L and Y21F point mutations, respectively (underlined). The forward primer PET28-F anneals upstream of the polycloning site of the pET28(a)(+) vector. The first PCR was achieved using two primer pairs, PET28-F, Y21L-R (or Y21F-R) and Y21L-F (or Y21F-F), AppA156-R (described above), using the plasmid pETAppA156 (see above) as the template. The two resulting DNA fragments were mixed and then used as a template in a second PCR amplification using PET28-F and AppA156-R primers. The second PCR products were digested with *Nde*I and *Sac*I and ligated into *Nde*I−*Sac*I-cut pET28(a)(+). The resulting plasmids were named pETY21L and pETY21F for Y21L and Y21F mutant proteins, respectively.

The recombinant plasmids pETAppA156, pETY21L, and pETY21F were transformed into the *E. coli* host strain BL21(DE3) (Novagen) with the proteins overexpressed by induction with 0.5 mM isopropyl β-D-thiogalactopyranoside (IPTG) at 25 °C for 3 h. Further purification steps were the same as for the native His-tagged AppA as described previously (*3*). Luria broth medium was used in the presence of kanamycin at a concentration of 50 μg/mL. Molar extinction coefficients were calculated on the basis of the concentration of protein as measured by the Bradford method as described by the manufacturer (Bio-Rad Laboratories).

Spectroscopy. Ultraviolet and visible absorption spectra were obtained using a Beckman BU 640 spectrophotometer. Circular dichroism (CD) spectra were collected on a Jasco J-715 spectropolarimeter, equipped with an ultraviolet-sensitive photomultiplier tube detector. Samples in 10.1 mM Na_2HPO_4, 1.8 mM KH_2PO_4, 140 mM NaCl, and 2.7 mM KCl (pH 7.3) were adjusted to ∼125 μM (1.0 cm cell) for measurements in the visible region, ∼70 μM for near-UV (1.0 cm cell) (250−310 nm), and ∼20 μM (0.2 cm cell) for deep-UV (200−250 nm). Fluorescence measurements were obtained with a Perkin-Elmer LS 50 B luminescence spectrometer equipped with a Hamatatsu Model R2371 PMT. Samples were degassed by bubbling nitrogen through the solution for 15 min. Measurements were performed with concentrations of 50 μM in a 1 cm quartz cell equipped with an airtight Kontes stopcock. Photocycle illumination was performed with a 150 W halogen lamp (Model MKII; Nicon, Inc.) at an intensity 900 μmol m^{-2} s^{-1} for 30 s.

For nuclear magnetic resonance (NMR) spectroscopy, both WT and Y21F mutant AppA samples were exchanged to NMR buffers containing 50 mM Tris-d_6/acetate-d_3 buffer, 400 mM KCl, 0.1% NaN_3 and 90% ^2H_2O. Uncorrected pHs (p^2H) of the NMR buffers were 6.8. Deuterium exchange for all exchangeable protons was accomplished by centrifugation with a 20-fold excess amount of the NMR buffers using VIVASPIN-2 (Saltrius Co. Ltd.). Concentrated NMR samples were further immersed in NMR buffers overnight at 310 K. Both protein samples for NMR experiments were set at 0.1 mM and then transferred into Shigemi NMR tubes (Shigemi Co. Ltd.). All NMR spectra were recorded on a Bruker DRX-500 spectrometer operating at 500.03 MHz ^1H frequency with the temperature of the NMR samples maintained at 310 K. The residual water signals were suppressed by a Watergate pulse sequence with 1.2 s repetitive time, respectively.

Laser flash photolysis experiments were performed using a previously described apparatus (*8*). A nitrogen-pumped dye laser provided pulsed excitation of the sample at 445 nm. Transient kinetics were monitored at various wavelengths using a tungsten−halogen lamp passing through a monochromator.

Gel Filtration Chromatography. AppA samples were preincubated at 25 °C for 5 min under dark or high-light (900 μmol m^{-2} s^{-1}) conditions and then gel fractionated under dark or illuminated conditions with the column illuminated during fractionation. Typically, a 0.08% column volume of protein was size fractionated on a prepacked Sephacryl S-200 HR (16/60) column (Pharmacia Biotach) equilibrated with 25 mM Tris-HCl (Ph 8.0), 75 mM NaCl, and 25 mM KCl. Fractions (1.0 mL) were collected with eluted proteins identified by absorption at 280 nm.

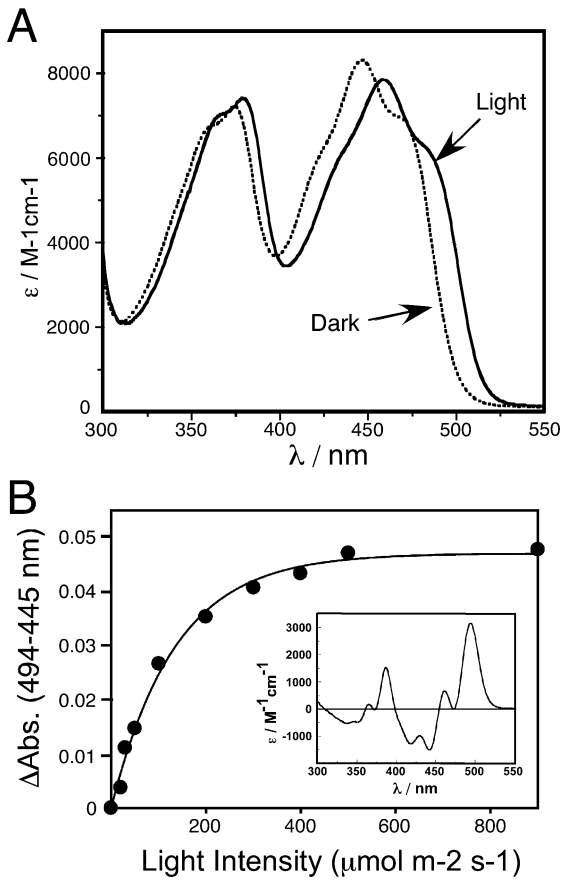

FIGURE 1: Ultraviolet and visible absorption spectra of the FAD-binding domain of AppA. (A) Absorption spectra of the dark-adapted and light-excited (for 30 s at 900 μmol m^{-2} s^{-1}) FAD-binding domain of AppA. (B) A fluence response curve for the photocycle of the FAD-binding domain of AppA that was generated by plotting the difference between 495 and 445 nm peaks in the light-excited minus dark difference spectrum versus exciting light intensity. Inset: Light-excited minus dark (for 30 s at 900 μmol m^{-2} s^{-1}) difference spectrum of the FAD-binding domain of AppA.

RESULTS

Spectroscopic Analysis of AppA156. A previous study established that the FAD-binding domain of AppA was significantly more soluble than full-length AppA (*5*). To perform detailed analysis of the AppA photocycle, we therefore analyzed a truncated 156 amino acid version of AppA (AppA156) that lacked the Cys-rich carboxyl-terminal domain. The electronic absorption spectrum of dark-adapted (>30 min prior to spectral analysis) AppA156 exhibits two broad flavin features centered at 365 and 445 nm (Figure 1A). The lower energy absorption band displays three distinct transitions separated by ~1020 cm^{-1}, which have previously been attributed to vibronic coupling of a ring mode of the isoalloxazine chromophore to the electronic transition (*9*, *10*). Upon excitation with 900 μmol m^{-2} s^{-1} of white light (or an Ar$^+$ laser operating at $\lambda = 457$ nm and 30 mW), there is a significant red shift observed in the position of both features, resulting in maxima at 371 nm and at 460 nm (Figure 1A). The low-energy transition shows a 15 nm red shift, with no disruption of the vibronic progression. Isosbestic points at 377, 398, and 454 nm are also observed upon conversion of the dark form to the light-adapted state. These spectral characteristics are identical to those observed with full-length AppA (*3*).

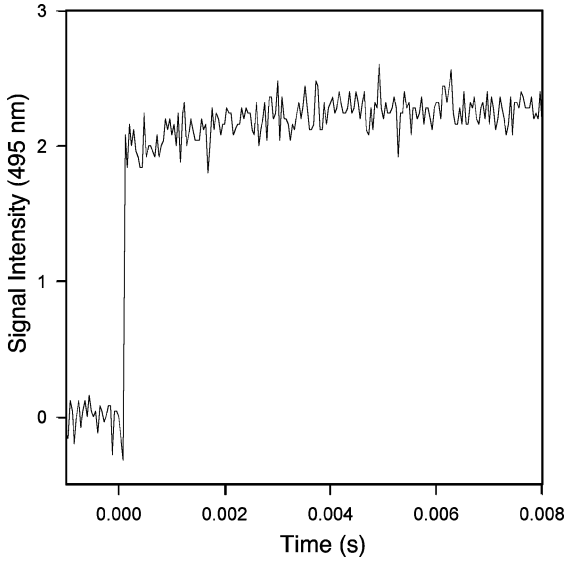

FIGURE 2: Flash-induced absorbance change in the FAD-binding domain of AppA monitored at 495 nm.

The light-excited minus dark-adapted difference spectrum of AppA156 (Figure 1B, inset) reveals negative features at 336, 352, 418, and 442 nm and positive peaks at 365, 387, 461, and 495 nm. Analogous spectral shifts in the visible region have been reported upon ligand and/or substrate binding to other flavoproteins (*11*−*16*). Differing mechanisms have been proposed to account for these observed spectral profile variations, including $\pi-\pi$ stacking (*16*), interactions of keto groups with the π-system of the flavin ring (*14*), and H-bonding at the O5 and N5 positions of the alloxazine ring (*15*).

A fluence response curve for the photoinduced spectral shift was obtained by generating a series of light-excited minus dark difference spectra from samples that were exposed to different light intensities (Figure 1B, inset). This analysis indicates that the light intensity needed for half-saturation of the photocycle is ~100 μmol m^{-2} s^{-1}, which is indistinguishable from that observed with full-length AppA (*3*). AppA156 and full-length AppA also both undergo decay from the blue-light-excited and red-shifted spectrum back to the ground state over a 30 min period with a calculated half-life of 15 min (data not shown). The similarity in the spectral features of full-length and AppA156 indicates that the photocycle reaction of AppA is achieved solely within the N-terminal FAD-binding domain and is directly related to excitation of the flavin chromophore.

The kinetics of photoproduct formation during the AppA photocycle was followed by measuring the rise in absorbance at 495 nm upon laser flash excitation at $\lambda = 445$ nm. As shown in Figure 2, biphasic kinetics were observed after single flash irradiation as indicated by a rapid initial rise of OD_{495} ($\tau_{1f} < 1$ μs; $k_{1f} > 10^6$ s^{-1}) followed by a less pronounced slow phase ($\tau_{2f} = 5$ ms; $k_{2f} = 690$ s^{-1}). The kinetics profile is also observed for the decrease in OD_{435} (data not shown), consistent with the bleaching at 435 nm observed in the difference spectrum (Figure 1B, inset). These results clearly reveal that photoproduct formation within the FAD-binding domain is a biphasic process.

Evidence for Interaction between the Alloxazine Ring of FAD with an Aromatic Residue. Recent evidence suggests that AppA may be one member of a new family of flavin-

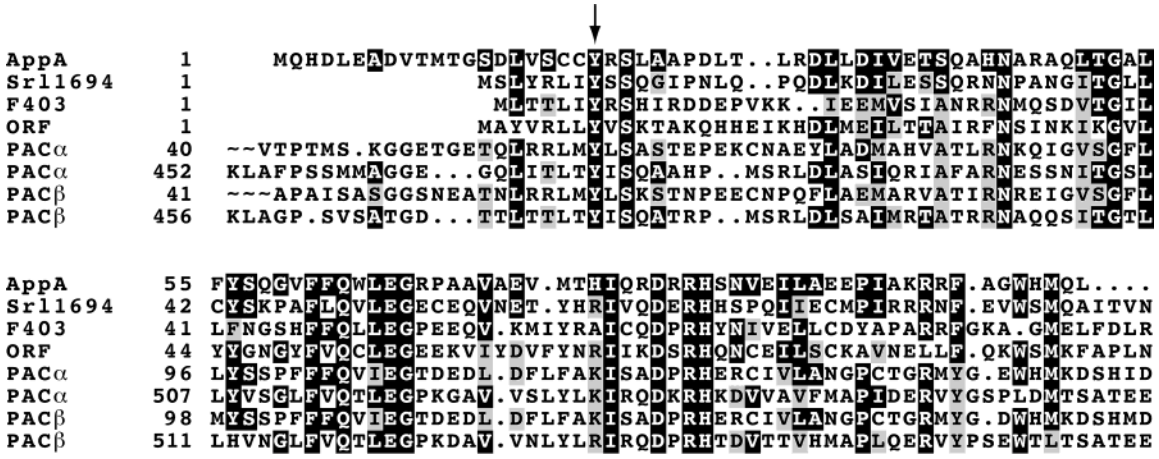

FIGURE 3: Amino acid sequence alignment of the primary structures of the FAD-binding domains from AppA, *Synechocystis* sp. Srl1694, *E. coli* F403, *Acinetobacter* sp. ORF1, and *E. gracilis* PACα and PAC*β* (accession numbers are AE000215, D90913, AF400583, AB031225, and AB031226, respectively). Conserved amino acids are shaded, and identical amino acids are printed white on black. Tyr21 is indicated with an arrow.

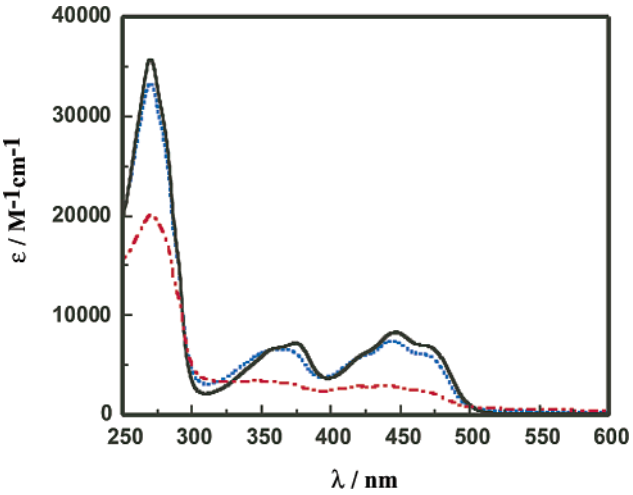

FIGURE 4: Comparison of the UV−visible spectra of FAD bound to AppA156 (black), Y21F (blue), and Y21L (red). Spectra were collected at 25 °C.

containing photoreceptors that possess significant homology in their first 130 amino acids (*3*, *4*, *17*). Alignment of five members of this family (Figure 3) reveals 30−35% similarity to the 130 amino acids at the amino terminus of AppA with the presence of a conserved tyrosine at position 21 (Tyr21). Since tyrosine contains both aromatic and H-bonding characteristics, we addressed whether Tyr21 may have a role in the binding of FAD as well as in the observed photocycle by constructing Phe and Leu mutations at this position (designed as Y21F and Y21L, respectively). AppA156 proteins containing the Y21L or Y21F mutation were then overexpressed, purified from *E. coli*, and spectrally compared to wild-type AppA156.

The UV−visible spectra of the Y21F and Y21L mutant AppA proteins show marked changes of flavin absorption relative to dark-adapted wild-type AppA156 (Figure 4). The wild-type protein has three transitions with peaks at $\lambda = 270$ nm ($\epsilon = 35800$ M^{-1} cm^{-1}), $\lambda = 366$ nm ($\epsilon = 7100$ M^{-1} cm^{-1}), and $\lambda = 446$ nm ($\epsilon = 8500$ M^{-1} cm^{-1}). The 270 nm peak is derived from spectral contributions from the two Trp and two Tyr aromatic residues ($\lambda = 270$ nm, $\epsilon \sim 13000$ M^{-1} cm^{-1}) as well as from the flavin cofactor ($\lambda = 270$ nm, $\epsilon \sim 22800$ M^{-1} cm^{-1}), while the lower energy transitions are derived solely from the flavin cofactor. Upon mutation of Tyr21 to Phe, all three transitions decrease in intensity ($\epsilon_{270} = 33300$ M^{-1} cm^{-1}, $\epsilon_{359} = 6700$ M^{-1} cm^{-1}, $\epsilon_{444} = 7500$ M^{-1} cm^{-1}). There is also a blue shift observed in the two low-energy flavin transitions ($\lambda_{max} = 359$ nm and $\lambda_{max} = 444$ nm). The decrease in the intensity of the 270 nm peak can be accounted for by replacement of Tyr ($\epsilon_{274} \sim 1440$ M^{-1} cm^{-1}) with a Phe residue ($\lambda_{max} = 257$ nm, $\epsilon \sim 220$ M^{-1} cm^{-1}), as well as from an increase in the hydrophobic nature of the flavin-binding pocket (*9*). In contrast, substitution of Tyr21 with a Leu residue results in dramatic changes in the electronic spectrum with the flavin peaks which are blue shifted and significantly reduced in intensity ($\lambda_{max} = 359$ nm, $\epsilon = 3500$ M^{-1} cm^{-1}; $\lambda_{max} = 438$ nm, $\epsilon = 3100$ M^{-1} cm^{-1}). The intensity of the flavin transitions is not altered after the addition of 10 molar equiv of $KHSO_5$ (data not shown), thereby indicating that the diminished extinction of the flavin transitions in Y21L is not a result of altering the redox state of the flavin. Additionally, the 270 nm peak in Y21L has lost considerable intensity ($\epsilon_{270} = 20100$ M^{-1} cm^{-1}), which cannot be accounted for by replacement of Leu for the Tyr residue. Since the 270 nm absorption band derives from the extinction of both the flavin and the remaining aromatic residues, the overall extinction attributable to the flavin can be estimated by subtracting the component derived from the protein ($\epsilon_{270protien} \sim 2\epsilon_{Trp} + \epsilon_{Tyr} \sim 11540$ M^{-1} cm^{-1}), yielding a flavin extinction of ~21500 M^{-1} cm^{-1} for the Y21F and ~8500 M^{-1} cm^{-1} for the Y21L mutant protein. If one assumes no changes in the intensity of the 270 nm flavin transition upon substitution of Leu for Phe, it can be calculated that only ~40% (8500/21500) of the Y21L protein contains the flavin cofactor. This value is consistent with the decrease in the intensity of the 440 nm peak ($\epsilon_{444} = 7500$ M^{-1} cm^{-1} for Y21F and $\epsilon_{438} = 3100$ M^{-1} cm^{-1} for Y21L), which also indicates that Y21L has only ~40% bound FAD. It is also clear that the flavin-binding pocket becomes more hydrophobic upon substitution of Leu for Phe as evidenced by the blue-shifted low-energy flavin transitions. While a change of this nature could cause a decrease in the intensity of the three flavin transitions, the magnitude of the decrease in intensity is much too large to simply be attributable to these effects (*9*). Instead, it appears that while the side chains

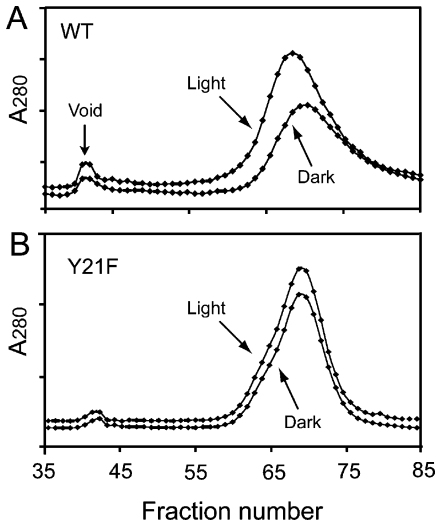

FIGURE 5: Size exclusion chromatography of the FAD-binding domain of AppA (A) and its Y21F mutant protein (B) in the dark and after irradiation for 5 min with white light (900 μmol m^{-2} s^{-1}).

of Tyr and Phe both provide a favorable and necessary environment for FAD binding, the substitution of the Leu aliphatic side chain results in a decrease in the binding affinity for FAD.

The AppA Photocycle Involves a Change in the Tertiary Structure. Size exclusion chromatography was performed with dark and light-excited AppA156 to establish whether excitation of the flavin results in a conformational change in the protein. In this experiment, AppA156 was preincubated under dark or high-light conditions and then subjected to chromatography also under dark or illuminated conditions. As shown in Figure 5A, dark-adapted wild-type AppA156 exhibited an elution profile of ~35 kDa (fraction 69) which was clearly distinguishable from an ~37 kDa (fraction 67) elution profile exhibited by light-excited AppA156. The different chromatographic features were highly reproducible, indicating that light excitation of the chromophore caused a stable conformational change in AppA156 that increases its Stokes radius and/or its dynamics. Additionally, the Y21F mutant protein, which does not undergo a light-induced spectral shift, exhibits an ~35 kDa elution profile under both dark and illuminated conditions (Figure 5B).

The far-UV (200−260 nm) CD spectrum of dark-adapted wild-type AppA (Figure 6A) reveals the presence of approximately 60% α-helix secondary structure as based on comparison to poly-L-lysine standards of known solution structures (*18*). This degree of helicity is retained in the Y21F and Y21L mutant proteins (Figures 6A), indicating that the loss of the photocycle in Y21F and Y21L is not a result of changes in the secondary structure caused by the Phe or Leu point mutations. From these data, it can be further concluded that the observed decrease in FAD binding of the Y21L mutant protein is not a result of a large change in the secondary structure of the mutant protein. In contrast, a comparison of the CD spectra of the flavin chromophore across the mutant series (Figure 6B) demonstrates a perturbation of the symmetry relationships between the isoalloxazine chromophore and either the ribityl side chain or the surrounding protein environment (*19*, *20*). Together, these results clearly indicate that mutation of Y21 only results in a local change in the flavin microenvironment.

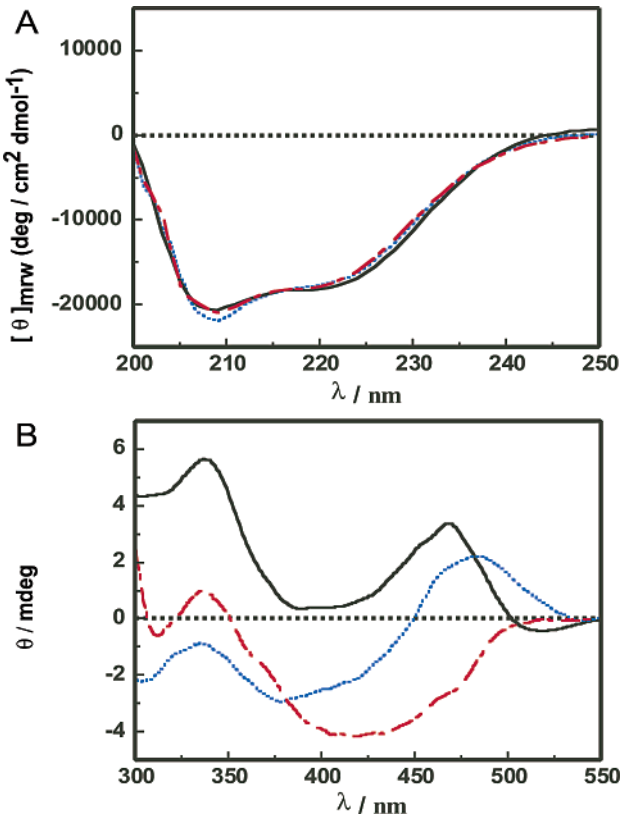

FIGURE 6: CD spectral analysis of wild-type, Y21F (red), Y21L (blue), and AppA156 proteins (black) in the 200−250 nm (A) and 300−550 nm (B) regions.

Photochemical excitation of the flavin in wild-type AppA156 (λ = 457 nm or λ > 300 nm) induces a slight increase in the percentage of random coil within the protein as indicated by the decrease in CD intensity at 220 nm and increase in the band at 201 nm (*18*) (Figure 7C). The features observed in the mid-UV region of the spectrum (Figure 7B) remain largely unchanged, with only a small increase in intensity of the two positive Cotton features at 289 and 253 nm. The increase in intensity of the peaks in the visible and mid-UV regions suggests that the overall tertiary structure is retained in light-excited AppA156 with only a minor perturbation of total chirality. Excitation of wild-type AppA156 also induces a slight increase in the intensities of the flavin transitions at 390, 468, and 488 nm in the CD spectrum (Figure 7A). These features correlate well with the red shift observed in the absorption spectra upon excitation. The light-induced spectral changes are reversible, with a recovery of the original features and intensities following 30 min dark incubation after initial exposure to light.

The Y21F Mutation in AppA Disrupts π−π Stacking Interactions. A comparison of expanded ^{1}H NMR spectra for wild-type and Y21F AppA156 proteins for both the aromatic and methyl regions is given in Figure 8. Since protons in these samples were carefully exchanged with deuterium in the NMR buffer, the spectral pattern observed in the aromatic region is representative of only the two Tyr, two Trp, four His, and seven Phe that are present in AppA156, in addition to those arising from the flavin ring itself. A comparison of the spectral pattern in the aromatic region between the WT AppA156 and the Y21F mutant demonstrates few changes in the peak positions, relative intensities, and the overall spectral topology, indicating that

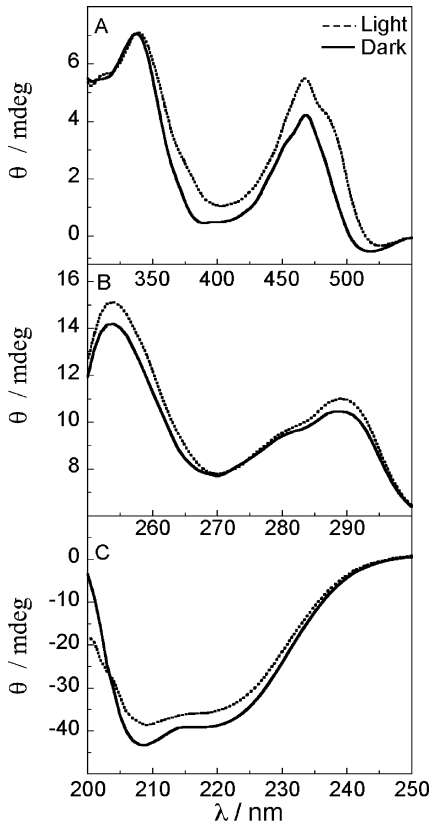

FIGURE 7: Effect of photolysis on the CD spectrum of wild-type AppA156 in the 200−250 nm (A), 250−300 nm (B), and 300−550 nm (C) regions. Spectra were collected at 25 °C with irradiation of photoexcited samples involving exposure to 900 μmol m^{-2} s^{-1} of white light for 30 s.

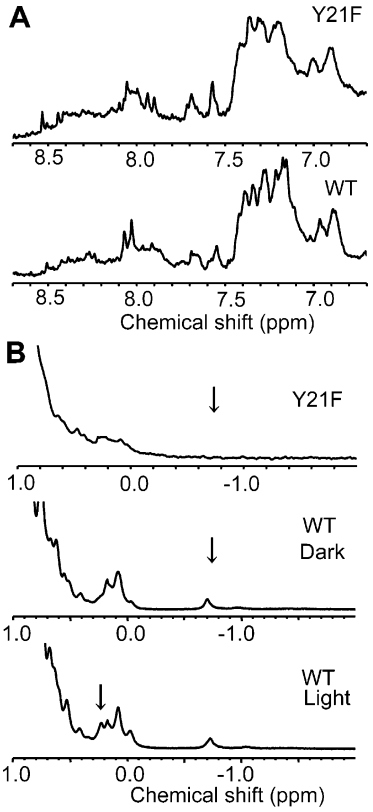

FIGURE 8: Comparison of the expanded ^{1}H NMR spectra for the aromatic (A) and the methyl (B) regions of the WT and the Y21F mutant AppA proteins. Both samples are dissolved in a deuterated buffer system (see Experimental Procedures) and are kept in the dark prior to NMR analysis (11 T).

the environment of the aromatic residues in Y21F is very similar to that observed for WT AppA156. The parallel nature of these spectra suggests that the substitution of Phe for Tyr at this position induces only local structural changes in the protein, further supporting the CD analysis. In contrast, the NMR spectra of WT and Y21F AppA156 exhibit remarkable differences at the −0.8 and 0.2 ppm region of the spectrum (Figure 8B). A number of resolved, but closely spaced, methyl resonances are observed in this region for both the light- and dark-adapted AppA156 that are absent in the Y21F spectra. In general, upfield-shifted methyl resonances are the result of ring current effects derived from neighboring aromatic residues in close spatial proximity to the NMR active nucleus (*21*−*23*). The spectral discrepancy between WT and Y21F AppA156 indicates that the wild-type protein contains significant stacking interactions that are lost upon substitution of Phe for Tyr. Overall, we estimate that there are four methyl resonances involved in these structural changes. Upon exposure of WT AppA156 to light, an increase in the number of resolved resonances at 0.2 ppm is observed, indicating that the protein environment in the vicinity of these specific methyl groups has been perturbed by photoexcitation. Given the changes in the flavin absorption (Figure 4) and CD (Figure 6D) spectra upon Y21F mutation, it is likely that the resonances from the methyl groups of FAD are among those shifted in the ^{1}H NMR spectra of AppA156.

Fluorescence Analysis of the AppA Photocycle. Fluorescence analysis of light- and dark-adapted AppA156 was undertaken to assay for perturbations in the flavin-binding pocket and in the protein structure overall. Exposure of WT AppA156 to light (λ = 457 nm or λ > 300 nm) results in significant quenching of the fluorescence from FAD with only 18% of the total intensity observed with the dark-adapted protein (Figure 9A). A 10 nm red shift in the flavin emission maximum is also observed, which is comparable in magnitude to the red shift of the UV−visible spectrum of the flavin that occurs upon photoexcitation. However, the excitation spectra for both the light- and dark-adapted fluorescence signals yield profiles that match the dark-adapted AppA156 absorption spectrum. Together, these results demonstrate that, after exposure to light, two forms of AppA156 are present in solution: residual dark-adapted AppA156, which is the primary contributor to the fluorescence intensity, and light-adapted AppA156, which exhibits very little fluorescence intensity and a red-shifted fluorescence maximum.

In contrast to the quenching of flavin emission, the fluorescence from tryptophan is quenched only slightly, retaining 88% of the dark-adapted intensity (Figure 9B). While variations in tryptophan fluorescence suggest minor changes in the protein structure, the exact origin of the quenching is complicated by the presence of two tryptophan residues in AppA156, both of which combine to yield the observed fluorescence intensity. Interestingly, recovery kinetics of the FAD (Figure 9C) and tryptophan fluorescence emissions (Figure 9D) are both biphasic, having rate constants on the order of 10^{-5} [k_{1ra} = (1.07 ± 0.02) × 10^{-5} s^{-1} for FAD and k_{1rb} = (3.81 ± 0.03) × 10^{-5} s^{-1} for Trp] and 10^{-3} s^{-1} [k_{1ra} = (1.91 ± 0.01) × 10^{-3} s^{-1} for FAD and

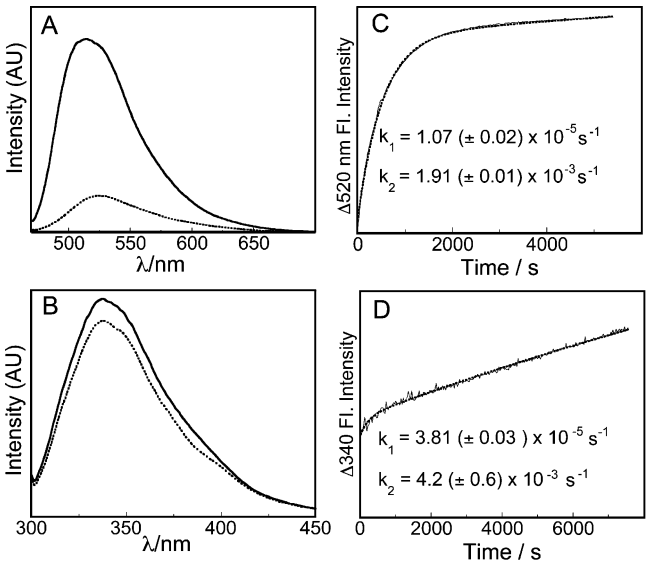

FIGURE 9: Effect of photoexcitation of AppA156 on fluorescence emission spectra and recovery kinetics. (A) Emission of FAD (λ_{ex} = 450 nm) from dark-adapted (—) and light-excited AppA156 (- - -). (B) Tryptophan fluorescence emission (λ_{ex} = 290 nm) from dark-adapted and (—) and light-excited (- - -) AppA156. (C) Experimental (—) and fit (- - -) of the fluorescence recovery kinetics of FAD by measuring the change in emission at 520 nm. (D) Experimental (—) and fit (- - -) of the tryptophan fluorescence recovery kinetics by measuring the change in emission intensity at 340 nm. Spectra and kinetics were measured at 25 °C under anaerobic conditions. Light excitation of AppA156 involved exposure of the sample to 900 μmol m^{-2} s^{-1} of white light for 30 s.

$k_{2rb} = (4.2 \pm 0.6) \times 10^{-3}$ s^{-1} for Trp]. Because distinct rate constants are observed for each fluorophore for both the "fast" and "slow" phases of the recovery, it is clear that the two quenched fluorophores are not directly interacting, thereby ruling out energy-transfer mechanisms as a means of tryptophan quenching. Furthermore, from the recovery kinetics it is apparent that the fast phase is much more pronounced for the flavin (recovering ~90% of the dark-adapted intensity for FAD and only ~20% of the Trp intensity), while the slow phase dominates the recovery of the tryptophan fluorescence (recovering ~80% of the dark-adapted intensity for Trp and only ~10% of the FAD intensity). These results indicate that the fast phase of the recovery more greatly reflects changes in the flavin environment, while the slow phase of the kinetics reflects a more extended conformational alteration affecting the fluorescence of the tryptophan(s). As a result, it can be concluded that, analogous to the formation kinetics (Figure 2), there are two phases of the recovery of AppA156 to the dark-adapted state (Figure 9C,D), affecting both the local environment of the FAD and the extended protein conformation.

Fluorescence excitation of either dark- or light-excited Y21F or Y21L mutant proteins also has no effect on the intensity of either the FAD or Trp fluorescence (data not shown). This is consistent with the observation that these mutant proteins do not undergo a photocycle or a change in shape as assayed by chromatography.

DISCUSSION

Spectral Features of the AppA Photocycle. In this study, we have characterized a flavin photocycle in the newly identified blue-light photoreceptor AppA. Consistent with a previous report (*5*), we found that a truncated version of AppA containing only the first 156 residues (AppA156) effectively binds FAD and that this domain exhibits a blue-light-dependent photocycle that is indistinguishable from that observed with full-length AppA.

Light-adapted AppA156 is characterized by a red shift of the absorption spectrum relative to dark-adapted AppA156. Light excitation also leads to quenching of both the FAD and Trp fluorescence and a perturbation of $\pi-\pi$ stacking interactions. A red shift in the absorption spectrum and quenching of fluorescence can be attributed to either H-bonding, π-stacking, or an increase in the solvent exposure of FAD. An increase in solvent exposure is not a viable explanation because this would only partially quench the emission (by ~50%) and would also result in an increase in the intensity of the 445 nm absorption band with an accompanying decrease in the resolution of the vibronic fine structure (*9*). Since these characteristics do not occur, there must be another explanation for the observed photocycle. One possibility is that an increased H-bonding interaction at N5 may be responsible for the changes in the fluorescence and absorption spectra that are observed upon photochemical excitation of AppA. This supposition is based on the observation that emission from flavin derivatives without the ribityl side chain is quenched in acidic media (*9*, *24*) and that comparable red shifts in the absorption spectra have been attributed to H-bonding interactions at N5 of the flavin ring (*15*, *25*−*26*). The presence of $\pi-\pi$ stacking interactions in the dark-adapted state and perturbations of the interaction in the light-adapted state also suggest an influence of stacking interactions on the fluorescence of light-adapted AppA156. A potential mechanism to account for differing degrees of quenching derived from stacking interactions could therefore involve a change in the relative orientation of the involved π-systems (*27*−*29*).

If the fluorescence quenching is a result of the altered relative orientation or distance of the flavin isoalloxazine ring π-system with respect to an aromatic stacking partner, then photochemical excitation of the flavin could cause a shift of the chromophore within the binding pocket. Indeed, semiempirical calculations demonstrate that photoexcitation can lead to an increase in electron density at the N5 position of the isoalloxazine ring (*30*, *31*) that can be correlated with an increase in proton affinity to N5 upon photochemical excitation (*32*, *33*). Furthermore, it is known that the presence of H-bonding interactions at N5 can act to lower the energy of the lowest unoccupied molecular orbital (LUMO) of flavins (*25*, *34*). This has been shown to result in spectral red shifts in flavoenzymes (*15*) that are similar to those observed with photoexcited AppA. Thus, excitation of the flavin could cause an increase in the basicity at N5 that induces a local structure change within the flavin-binding pocket that ultimately leads to extended global conformational changes in the protein. A mechanism of this nature is supported by the formation kinetics of the light-adapted AppA156 which demonstrates a biphasic rise in the absorbance at 498 nm, where the fast process is attributable to an excited-state event at the flavin ($k_{1f} > 10^6$ s^{-1}) and the slow process is indicative of an extended conformational change of the protein ($k_{2f} = 690$ s^{-1}) (Figure 2).

Mutation at Tyr21 Changes the Flavin-Binding Pocket. On the basis of homology present in putative flavin-binding

domains that were identified by a database search for homologous proteins, a conserved Tyr residue at position 21 and a Ser at position 23 were identified as potential participants in the observed photocycle. The hydroxyl group of Tyr is capable of H-bonding with the flavin chromophore, while the aromatic ring of Tyr can form π-stacked complexes with the isoalloxazine ring of FAD. The conserved Ser residue at position 23 is also capable of H-bonding and forming fluorescence quenching interactions with FAD (*35*). However, in contrast to mutating Tyr21, which results in proteins that properly fold and are capable of binding FAD, mutations in Ser32 form insoluble protein (data not shown). Thus, although Ser23 is a possible contributor to the spectroscopic features of AppA, our studies have focused on the role of Tyr21 in affecting the activity of the photocycle.

A comparison of the CD spectroscopic properties of dark-adapted WT AppA156 relative to the Y21L and Y21F mutants reveals that all three proteins exhibit conserved global protein structures with a 40/60 mix of random coil to α-helix (Figure 5A). A comparison of the absorption spectra of wild-type and mutant AppA156 indicates that the mutations do lead to a change in the local flavin environment. While the intensity of the low-energy absorption band remains relatively constant, there is a small blue shift in the Phe mutant spectra relative to the wild-type spectra (Figure 3). A blue shift is also observed in the high-energy band, reflecting an increase in the hydrophobic nature of the flavin environment upon going from Tyr to Phe. Upon mutation of Tyr to Leu a dramatic drop in the intensity of all three peaks is observed, consistent with a decreased affinity for FAD. Moreover, a large blue shift is observed in both of the low-energy transitions, indicating an increase in the hydrophobic nature of the flavin-binding pocket. Alterations of the flavin environment are also observed in the CD spectrum of the flavin region (Figure 5B). Since the sign and relative magnitude of the CD signals from the flavin chromophore only reflect changes in the symmetry relationships between the isoalloxazine ring and either the ribityl side chain or the orientation of the residues surrounding the chromophore (*19*, *20*), detailed information about the local structural change cannot be derived from the CD data. However, from these data, it is clear that a substantial change in the orientation of the flavin chromophore is observed upon mutation of Tyr21 with respect to the surrounding residues and/or the ribityl side chain.

NMR analysis of dark-adapted AppA156 also shows the presence of numerous well-resolved high-field signals in the methyl region (Figure 7B) which are characteristic of ring current effects derived from interactions between the FAD and a spatially close aromatic residue involved in $\pi-\pi$ stacking interactions (*21*−*23*). These high-field signals are absent in the Y21F mutant protein. Given the conservation of the global protein structure and the local changes in the flavin-binding pocket upon mutation, it is reasonable to conclude that $\pi-\pi$ stacking interactions exist between the isoalloxazine ring of the flavin and the aromatic ring of Tyr21. Furthermore, the conservative nature of the Y21F mutation implicates direct H-bonding interactions between the hydroxyl group in Tyr21 and the flavin ring, which presumably facilitate proper stacking interactions between the flavin isoalloxazine ring and the aromatic ring in Tyr21.

The AppA Photocycle Initiates a Global Conformational Change. Even though the CD and NMR analyses of dark-adapted and photoexcited AppA156 indicate that there are only small changes in the polypeptide secondary structure, the chromatography results do reveal that significant light-induced changes in the protein structure do occur. Two possible explanations (or both) may be considered for the action of AppA156 upon photoexcitation. One is that there are two (or more) distinct domains in AppA156 that are tethered by a flexible hinge region with the protein favoring one structural conformation in the dark-adapted state and a different conformation in the light-excited state. The other idea considers the conformational flexibility or entropy change of this domain upon photoexcitation, in which dynamical change of this domain regulates the activity of AppA. Such dynamical regulation of some protein activities has been suggested recently, including the LOV domain, the flavin-binding domain of the plant blue-light receptor, phototoropin (*36*, *37*). Clearly, more detailed crystallography and solution spectroscopy of this domain are necessary to test this model, and these studies are currently underway in the authors' laboratories.

The flash excitation experiments show that light-induced formation of the stable red-shifted form of the protein involves a biphasic reaction (as monitored by an increase in OD_{498}) with a fast phase having a rate constant of $>10^6$ s^{-1} and a slow phase at 690 s^{-1} (Figure 8). The kinetics for the recovery of the light-adapted AppA156 to the dark-adapted protein is also biexponential with recovery of Trp and FAD fluorescence grouped into fast (k_{1r} $\sim 10^{-5}$ s^{-1}) and slow events (k_{2r} $\sim 10^{-3}$ s^{-1}). As a result, it can be concluded that there are two phases of both the formation of light-adapted AppA156 and the subsequent return to the dark-adapted state which affect both the local environment of the FAD and (but to a lesser extent) the extended protein conformation. We suspect that the fast phase of the formation kinetics involves local changes in electron density that strengthen a H-bonding interaction at the N5 position of the flavin ring. Although it is likely that additional H-bonding interactions of the flavin may change upon excitation, the spectral red shift clearly implicates altered hydrogen bonding at N5 (*15*, *25*, *34*). A local flavin conformational change in the light-adapted protein presumably involves an increase in the proximity of the hydroxyl group in Tyr21 to the N5 position of the flavin (as discussed above), which leads to both a red shift of the flavin absorption spectrum through stabilization of the LUMO and a quenching of the FAD fluorescence (via a perturbation of the dark-state π-stacking interaction). This local change of the flavin orientation initiates a relatively slow "second phase" (Figure 8) of the formation of the red-shifted form of AppA, which is most likely related to changes in the molecular volume (Figure 4) of the protein rather than due to an electronic rearrangement of the flavin. The recovery kinetics follow the same general trend, having a fast phase which appears to be primarily localized at the flavin, while the slow phase more greatly affects residues not directly interacting with the flavin.

A viable description of the photocycle, consistent with all of the structural, spectroscopic, and kinetic data, suggests that there are initial light-induced alterations of hydrogen bond interactions of the flavin which subsequently lead to alterations in the relative conformation of distinct protein

domains. A conformational change of this type would not only affect the Stokes radius (and/or the dynamics) of the protein (Figure 4) but also affect the total chirality of AppA156 upon excitation (Figure 6B).

Concluding Remarks. A flavin photocycle reaction involving photoinduced alterations of H-bonding interactions of the flavin has not been observed in other flavoprotein photoreceptors. Indeed, the photochemical reaction of AppA is distinctly different from that observed in the flavin-binding domains of plant blue-light photoreceptors, phototropin and cryptochrome (*38*−*39*). In the case of phototropin, the photocycle has been found to involve the formation of a transient flavin−cysteinyl adduct (*40*−*42*). While details of blue-light sensing by cryptochrome are not clear, it is thought to involve the formation of a flavin radical (*43*). Although AppA, phototropin, and cryptochrome all use flavin as a blue-light-absorbing pigment, these proteins have very different flavin-binding domains. Thus, they appear to have independently evolved ways to use the blue-light-absorbing properties of flavin to transmit information on the intensity of blue light to control gene expression.

AppA is one of several proteins that exhibit considerable homology at their amino-terminal domain (1−110 amino acids) but no significant homology among their carboxyl-terminal regions. These proteins are derived from such diverse organisms as the cyanobacterium *Synechocystis* PCC6803, *Acinetobacter*, *E. coli*, and the alga *Euglena gracilis.* This suggests that members of the AppA family may contain common blue-light "input domains" with different sets of carboxyl-terminal "output domains". This would allow these proteins to control many different cellular processes in response to blue light. Although functions for most of these AppA-like proteins are unknown, the AppA-like protein isolated from *E. coli* has been shown to contain flavin (*5*). In addition, a blue-light avoidance response exhibited by *E. gracilis* was recently shown to involve two polypeptides of this family that are also known to bind flavin (*17*). Thus, this protein family appears to constitute flavin-bound photoreceptors that are present in diverse species of organisms.

REFERENCES

1. Briggs, W. R., and Huala, E. (1999) *Annu. Rev. Cell Dev. Biol. 15*, 33−62.
2. Lin, C. (2000) *Trends Plant Sci. 5*, 337−342.
3. Masuda, S., and Bauer, C. E. (2002) *Cell 110*, 613−623.
4. Gomelsky, M., and Kaplan, S. (1995) *J. Bacteriol. 177*, 4609−4618.
5. Gomelsky, M., and Kaplan, S. (1998) *J. Biol. Chem. 273*, 35319−35325.
6. Norrander, J., Kempe, T., and Messing, J. (1983) *Gene 26*, 101−106.
7. Wang, W., and Malcolm, B. A. (1999) *BioTechniques 26*, 680−682.
8. Tollin, G. (1995) *J. Bioenerg. Biomembr. 27*, 303−309.
9. Koziol, J. (1971) *Methods Enzymol. 18*, 253−285.
10. Webber, G., (1966) Intramolecular Complexes of Flavins, in *Flavins and Flavoproteins* (Slater, E. C., Ed.) pp 15−21, Elsevier, Amsterdam.
11. Zhou, Z., and Swenson, R. P. (1996) *Biochemistry 35*, 15980−15988.
12. Jung, Y. S., Roberts, V. A., Stout, C. D., and Burgess, B. K. (1999) *J. Biol. Chem. 274*, 2978−2987.
13. Pellett, J. D., Becker, D. F., Saenger, A. K., Fuchs, J. A., and Stankovich, M. T. (2001) *Biochemistry 40*, 7720−7728.
14. Gopalan, K. V., and Sirvastava, D. K. (2002) *Biochemistry 41*, 4638−4648.
15. Axley, M. J., Fairman, R., Yanchunas, J., Villafranca, J. J., and Robertson, J. G. (1997) *Biochemistry 36*, 812−822.
16. Rowland, P., Bjornberg, O., Nielsen, F. S., Jensen, K. F., and Larsen, S. (1998) *Protein Sci. 7*, 1269−1279.
17. Isekim, M., Matsunaga, S., Murakami, A., Ohno, K., Shiga, K., Yoshida, K., Sugai, M., Takahahi, T., Hori, T., and Watanabe, M. (2002) *Nature 415*, 1047−1051.
18. Greenfield, N., and Fasman, G. D. (1969) *Biochemistry 8*, 4108−4116.
19. Edmondson, D. E., and Tollin, G. (1971) *Biochemistry 10*, 113−123.
20. Shiga, K., Horiike, K., Nishina, Y., Otani, S., Watari, H., and Yamano, T. (1979) *J. Biochem. (Tokyo) 85*, 931−941.
21. Blanchard, L., Hunter, C. N., and Williamson, M. P. (1997) *J. Biomol. NMR 9*, 89−95.
22. . Kikuchi, J., Asakura, T., Hasuda, K., Ito, T., Ohwaku, K., Araki, H., and Williamson, M. P. (2000) *J. Biochem. Biophys. Methods 42*, 35−47.
23. Perkins, S. J., and Wuthrich, K. (1980) *J. Mol. Biol. 138*, 43−64.
24. Schreiner, S., Steiner, U., and Kramer, H. E. A. (1975) *Photochem. Photobiol. 21*, 81−84.
25. Niemz, A., Imbriglio, J., and Rotello, V. M. (1997) *J. Am. Chem. Soc. 119*, 887−892.
26. Breinlinger, E. C., Keenen, J., and Rotello, V. M. (1998) *J. Am. Chem. Soc. 120*, 8606−8609.
27. Bevers, S., Schutte, S., and McLaughlin, L. W. (2000) *J. Am. Chem. Soc. 122*, 5905−5915.
28. Pilch, D. S., Martin, M. T., Nguyen, C. H., Sun, J. S., Bisagni, E., Garestier, T., and Helene, C. (1993) *J. Am. Chem. Soc. 115*, 9942−9951.
29. Shirai, K., Matsuoka, M., and Fukunishi, K. (1999) *Dyes Pigments 42*, 95−101.
30. Heelis, P. F., Parsons, B. J., and Yano, Y. (1997) *J. Chem. Soc., Perkin Trans. 2*, 795−798.
31. Song, P. S. (1968) *Photochem. Photobiol. 7*, 311−313.
32. Arnaut, L. J., and Formosinho, S. J. (1993) *J. Photochem. Photobiol. 75*, 1−20.
33. Sharma, A., and Schulman, S. G. (1999) *Introduction to Fluorescence Spectroscopy. Techinques in Analytical Chemistry*, Wiley and Sons, New York.
34. Breinlinger, E. C., and Rotello, V. M. (1997) *J. Am. Chem. Soc. 119*, 1165−1166.
35. Mulrooney, S. B., and Williams, C. H., Jr. (1997) *Protein Sci. 6*, 2188−2195.
36. Young, M. A., Gonfloni, S., Superti-Furga, G., Roux, B., and Kuriyan, J. (2001) *Cell 105*, 115−126.
37. Crosson, S., Rajagopal, S., and Moffat, K. (2003) *Biochemistry 42*, 2−10.
38. Huala, E., Oeller, P. W., Liscum, E., Han, I.-S., Larsen, E., and Briggs, W. R. (1997) *Science 278*, 2120−2123.
39. Christie, J. M., and Briggs, W. R. (2001) *J. Biol. Chem. 276*, 11457−11460.
40. Salomon, M., Christie, J. M., Knieb, E., Lempert, U., and Briggs, W. R. (2000) *Biochemistry 39*, 9401−9410.
41. Crosson, S., and Moffat, K. (2001) *Proc. Natl. Acad. Sci. U.S.A. 98*, 2995−3000.
42. Swartz, T. E., Corchnoy, S. B., Christie, J. M., Lewis, J. W., Szundi, I., Brigss, W. R., and Bogomolni, R. A. (2001) *J. Biol. Chem. 276*, 36493−36500.
43. Lin, C., Robertson, D. E., Ahmad, M., Raibekas, A. A., Jorns, M. S., Dutton, P. L., and Cashmore, A. R. (1995) *Science 269*, 968−970.

BI030055O